

Influence of Charge Doping on Thermal Diffusivity of Double Perovskite $\text{Sr}_2\text{FeMoO}_6$ Studied by Mirage Effect

C. X. Zhao,¹ A. H. Luo,¹ X. J. Liu,^{1, 2} S. Y. Zhang,¹ and L. P. Cheng¹

Received July 1, 2003

Effects of charge doping on thermal diffusivity have been investigated in double perovskite ferromagnetic $\text{Sr}_{2-x}\text{La}_x\text{FeMoO}_6$ ($0 \leq x \leq 0.4$) by means of the mirage effect at 300 K (\ll the critical temperature $T_c \sim 420$ K). Substitution of the La^{3+} ions for the Sr^{2+} ions significantly increases the value of the thermal diffusivity from $0.39 \text{ cm}^2 \cdot \text{s}^{-1}$ at $x=0$ to $0.54 \text{ cm}^2 \cdot \text{s}^{-1}$ at $x=0.4$. The increased thermal diffusivity is ascribed to the extra itinerant electrons on the $\text{Mo}4d_{\downarrow}$ band.

KEY WORDS: charge doping; double perovskite; mirage effect; thermal diffusivity.

1. INTRODUCTION

Carrier doping in strongly correlated electron systems is a powerful tool to discover new phenomena and synthesize new materials. High- T_c superconducting cuprates and perovskite-structural manganites are the most celebrated examples. In the latter case, the parent complex LaMnO_3 is insulating and antiferromagnetic. A metallic and ferromagnetic behavior is promoted with substitution of the divalent Sr^{2+} ions for the trivalent La^{3+} ions. The generic features of magnetic and transport properties of this system are well understood in the framework of a double exchange (DE) mechanism, which includes the transfer of the e_g electrons (transfer integral t) and the strong Hund's rule coupling J between the local t_{2g} spins and the e_g electrons [1].

¹Institute of Acoustics and Lab of Modern Acoustics, Nanjing University, Nanjing 210093, P. R. China

²To whom correspondence should be addressed. E-mail: liuxiaojun@nju.edu.cn

Recently, transition metal oxides with ordered double-perovskite structure, $A_2M\text{MoO}_6$, $A_2M\text{ReO}_6$, and $A_2M\text{WO}_6$ (A is a rare-earth metal and M is a transition metal) currently attract considerable interest from the viewpoint of fundamental physics and technological applications to magnetoresistance devices [2, 3]. Among them, $A_2\text{FeMoO}_6$ ($A = \text{Ca}, \text{Sr},$ and Ba) is known to be ferromagnetic with a critical temperature T_c (~ 400 K) [3], which is higher than that of charge doped manganites, e.g., $T_c \sim 360$ K for $\text{La}_{0.6}\text{Sr}_{0.4}\text{MnO}_3$. In this system, Fe^{3+} ions ($3d^5$) behave as local spins, while the conduction band is occupied by the 4d electrons of Mo^{5+} ($4d^1$) ions [4]. Navarro et al. [5] investigated the effects of electron doping on the magnetic and structural properties in $\text{Sr}_2\text{FeMoO}_6$, and found a substantial reduction of the saturation magnetization M_s . They have ascribed the reduced M_s to the increased antisite disorder of the Fe and Mo ions due to substitution of La^{3+} ions for Sr^{2+} ions. Moritomo et al. [6] also observed the same behavior in the same system. By contrast, they interpreted the observed behavior in terms of the occupation of the doped electrons in the down-spin Mo4d band. On the other hand, from the viewpoint of thermal dynamics, the thermal diffusivity should be increased by the extra itinerant electrons in the Mo4d band, and decreased by the antisite disorder of the Fe and Mo ions. Therefore, investigation of the thermal properties may be a key to clarify the origin of the reduced saturation magnetization M_s . However, little work has been carried out on the thermal properties, i.e., thermal diffusivity and thermal conductivity of the double-perovskite system, especially for the influence of electron doping on the thermal properties.

Photoacoustic (PA) and photothermal (PT) techniques have been successfully applied to characterize the thermal properties of solids in the last decade [7]. In this paper, we measured the thermal diffusivity of the electron doped double perovskite $\text{Sr}_{2-x}\text{La}_x\text{FeMoO}_6$ ($0 \leq x \leq 0.4$) by means of the mirage effect at 300 K. The thermal diffusivity shows a gradual increase with an increase in the La doping concentration x , suggesting that the doped electrons occupy mainly the down-spin Mo4d band.

2. EXPERIMENT

The melt-grown crystals, $\text{Sr}_{2-x}\text{La}_x\text{FeMoO}_6$ ($0 \leq x \leq 0.4$), were made by the floating-zone method [5]. A stoichiometric mixture of commercial SrCO_3 , La_2O_3 , Fe_2O_3 , Mo, and MoO_3 was well ground, and pressed into a rod with a size of $\sim 5 \text{ mm} \times 100 \text{ mm}$ and sintered at 1200°C for 2 h in a flow of Ar gas. The crystal was grown at a feeding speed of $\sim 20 \text{ mm h}^{-1}$ in the Ar atmosphere. Black and shiny crystals, typically 4–5 mm in diameter and $\sim 20 \text{ mm}$ in length, were obtained. X-ray

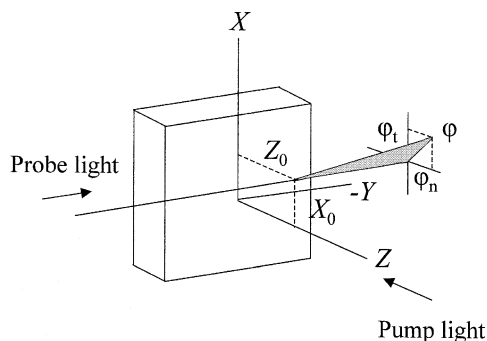


Fig. 1. Schematic diagrams of the geometric position of the probe and pump beams in the mirage technique.

diffraction (XRD) measurements and Rietveld analysis of the patterns indicate that the obtained crystals have a tetragonal ($I4/mmm$; $Z=2$) symmetry, consistent with previous reports [2, 3]. The antisite disordering of the Fe and Mo ions was estimated to be about 15% at $x=0$, and increased to 17% with increasing x to 0.4.

The thermal diffusivity measurement of $\text{Sr}_{2-x}\text{La}_x\text{FeMoO}_6$ is performed with the mirage method [7, 8]. As shown in Fig 1, an intensity-modulated laser beam irradiates perpendicularly the sample surface to cause local heating and hence the periodic temperature change. Another weak laser beam, acting as the probe beam, propagates parallel and adjacent to the sample surface. The periodic temperature at the sample–gas interface causes the periodic change of the refractive index gradient of a gas layer adjacent to the sample surface. Thus, the periodic beam deflection is consequently produced. In Fig. 1, Z_0 is the distance between the probe beam and the sample surface, X_0 is the distance between the pump and the probe beams, φ is the deflecting angle of the probe beam, φ_t is the deflection parallel to the sample surface, and φ_n is the deflection perpendicular to the sample surface.

In the mirage method [7], the thermal diffusivity is measured by searching the zero-crossing points of the in-phase component of the transverse mirage-effect deflection signal, which is used to determine the thermal wavelength. The signal was detected by a photodiode equipped in a lock-in amplifier. The phase of the lock-in amplifier was set so that the 90° phase points correspond to zero crossings of the in-phase signal. The distance x_0 between the two zero crossing points on both sides of the origin is given by

$$x_0 = d_0 + (\pi\alpha/f)^{1/2}, \quad (1)$$

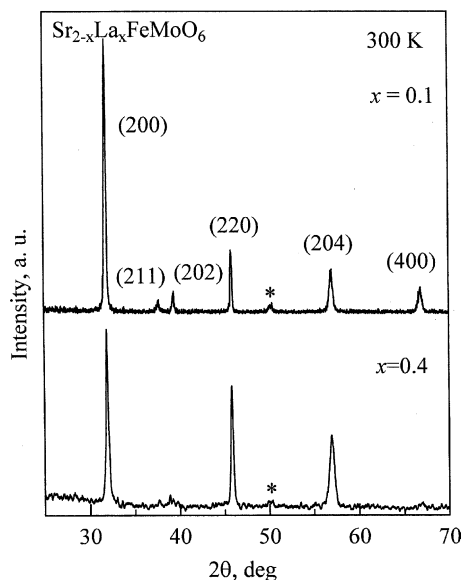


Fig. 2. XRD powder patterns of $\text{Sr}_{2-x}\text{La}_x\text{FeMoO}_6$ at 300 K: upper and bottom panels are for $x=0$ and 0.4, respectively. Peaks due to impurity SrMoO_4 are noted by *.

where d_0 is a distance on the order of the heating-beam diameter, f is the modulation frequency, and α is the thermal diffusivity of the sample. Thus, a plot of x_0 vs. the reciprocal of the square root of the frequency should have a slope given by $(\pi\alpha)^{1/2}$. The modulation-frequency range in the experiments was usually from 100 Hz to 4 kHz [8]. We calibrate the experimental system by the evaluation of the thermal diffusivity of Si, which is found to be $0.79 \text{ cm}^2 \cdot \text{s}^{-1}$. The systematic and statistical errors of the thermal diffusivity data are estimated to be $\pm 5\%$.

3. RESULTS AND DISCUSSION

Before describing details of the influence of electron doping on the thermal properties for $\text{Sr}_2\text{FeMoO}_6$, let us survey the variation of the structural and magnetic properties with substitution of La^{3+} for Sr^{2+} ions. Figure 2 shows the XRD patterns of $\text{Sr}_{2-x}\text{La}_x\text{FeMoO}_6$ powder at 300 K: the upper and bottom panels are for $x=0.1$ and 0.4, respectively. It shows that the samples have a small amount of an SrMoO_4 impurity phase, in accordance with previous reports [2, 3]. In both compounds, all XRD peaks except for the peaks of SrMoO_4 can be indexed according to the

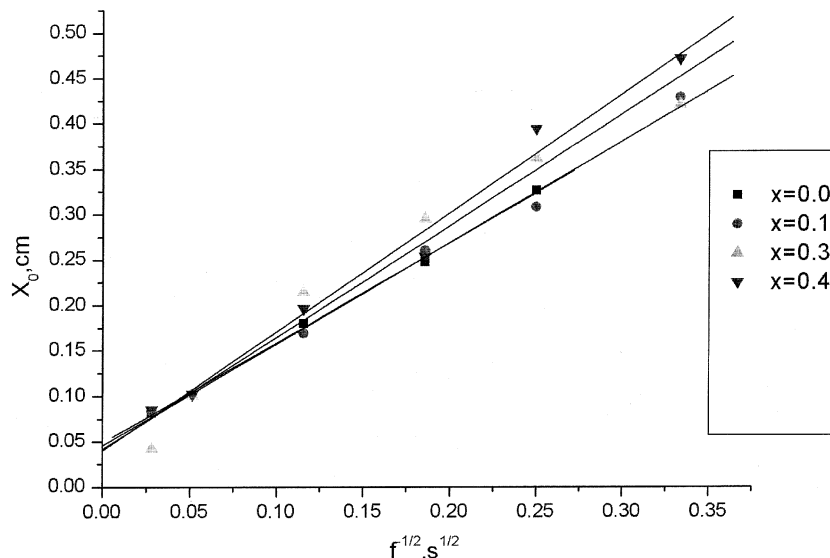


Fig. 3. Plot of x_0 vs. the reciprocal of the square root of the frequency f for $\text{Sr}_{2-x}\text{La}_x\text{FeMoO}_6$ ($0 \leq x \leq 0.4$). The straight lines represent the least-squares-fitted results.

space group ($I4/mmm$; $Z = 2$), indicating that there is no distinguished structure change with La substitution from $x = 0$ – 0.4 . We also measure the magnetization M for $\text{Sr}_{2-x}\text{La}_x\text{FeMoO}_6$ ($0 \leq x \leq 0.4$) at 50 K, and find that the M -value rapidly increases with external magnetic field H , and then is saturated when H is beyond 4 T. The saturation magnetization M_s decreases with increasing x : $M_s = 3.3 \mu_B$ at $x = 0$ and $M_s = 2.4 \mu_B$ at $x = 0.4$. Such a result is consistent with previous studies [5, 6].

In order to understand the origin of the depressed M_s upon La substitution, let us consider the variation of the thermal diffusivity with x . In Fig. 3, a plot of x_0 vs. the reciprocal of the square root of the frequency f is obtained by the mirage effect for $\text{Sr}_{2-x}\text{La}_x\text{FeMoO}_6$ ($x = 0, 0.1, 0.3$, and 0.4). The straight lines represent the least-squares-fitted results. Note that part of the line for $x = 0.1$ overlaps with that for $x = 0$. The obtained x dependence of the thermal diffusivity α for $\text{Sr}_{2-x}\text{La}_x\text{FeMoO}_6$ at 300 K is illustrated in Fig. 4a. With an increase of x from 0 to 0.4, the α -value gradually increases from 0.39 to $0.54 \text{ cm}^2 \cdot \text{s}^{-1}$. For comparison, we plot the x dependence of the M_s -values obtained at 50 K in Fig. 4b, which shows that the x dependence of the M_s has an opposite trend to that of the α -value. For magnetic materials, the thermal conductivity is usually written as a sum of three terms [9], similarly, the thermal diffusivity can also be written as $\alpha = \alpha_{\text{ph}} + \alpha_{\text{el}} + \alpha_{\text{sp}}$, where α_{ph} , α_{el} , and α_{sp} are the contributions from phonons, electrons and spin, respectively. The

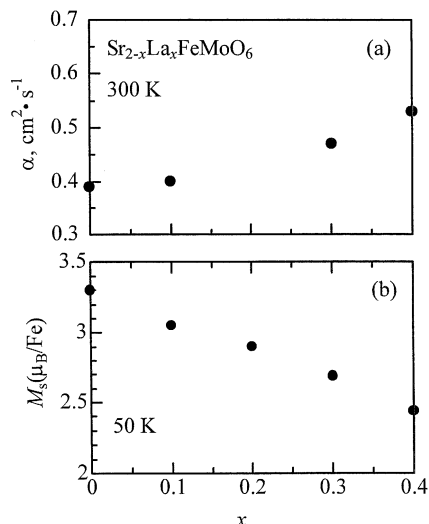


Fig. 4. La concentration x dependence of (a) the thermal diffusivity α at 300 K and (b) the saturation magnetization M_s at 50 K for $\text{Sr}_{2-x}\text{La}_x\text{FeMoO}_6$ ($0 \leq x \leq 0.4$).

α_{ph} -value should decrease with substitution of La^{3+} ions for Sr^{2+} ions, because the resultant mass and strain misfits should increase the phonon scattering. If the spin contribution α_{sp} is dominant, the thermal diffusivity should decrease due to the antisite disordering of Fe and Mo ions. Therefore, the increase of the thermal diffusivity with La substitution indicates the contribution of the electronic part α_{el} , i.e., the occupation of the extra itinerant electrons in the Mo4d band.

We further investigate the La concentration dependence of electric resistivity ρ for $\text{Sr}_2\text{FeMoO}_6$ in the temperature range 100–310 K. In Fig. 5, the compound at $x = 0$ shows a metallic behavior ($d\rho/dT > 0$) in the detected temperature range. With increasing x up to 0.4, the ρ -value shows a gradual decrease even if the metallic state remains, which is consistent with the increase of thermal diffusivity due to La doping investigated by the mirage effect.

It has been recently shown that the dominant magnetic interaction in $\text{Sr}_2\text{FeMoO}_6$ is ferromagnetic, and likely from DE interactions as found in the manganites [10]. Within the DE scenario, the ferromagnetic coupling between the local Fe^{3+} spins is mediated by the Mo4d band near the Fermi level E_F . Thus, M_s should increase with an increase in the itinerant electron density in the Mo4d band. However, this picture cannot account for the experimental data, i.e., the reduced M_s (see Fig. 4b). The structural

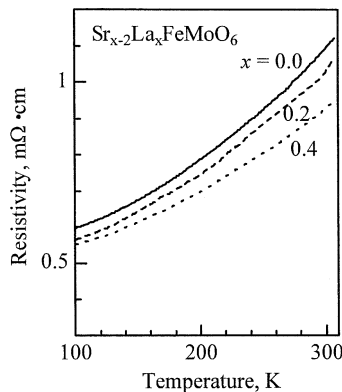


Fig. 5. Temperature dependence of resistivity ρ for $\text{Sr}_{2-x}\text{La}_x\text{FeMoO}_6$ ($x = 0, 0.2,$ and 0.4).

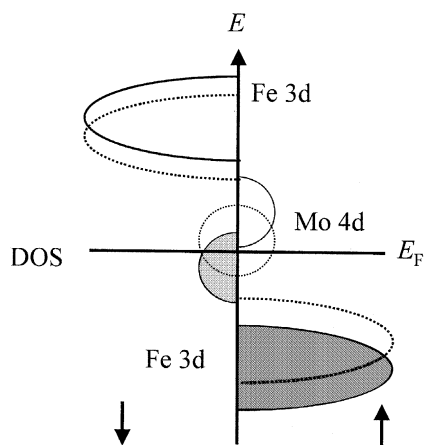


Fig. 6. Schematics for variation of density of state (DOS) in $\text{Sr}_2\text{FeMoO}_6$ in ferromagnetic phase: the solid one is proposed by Kanamori et al. and the broken one is normal. \uparrow and \downarrow represent the up-spin and down-spin states, respectively.

analysis also implies an enhanced M_s : the Fe–O–Mo bonds are closed upon La substitution and hence result in a larger hopping integral Fe–O–Mo of the itinerant electrons [5]. What is the origin of the depressed M_s ? Kanamori et al. [11] proposed an alternative model for the magnetism of $\text{Sr}_2\text{FeMoO}_6$. If the Fe^{3+} spins are ferromagnetically ordered, the hybridization between the Fe3d and Mo4d states pushes up (down) the up-spin

Mo4d_↑ (down-spin Mo4d_↓) states located between the Fe3d_↑ and Fe3d_↓ levels, as shown in Fig. 6. Then, the electrons near the E_F level transfer from the Mo4d_↑ band to the Mo4d_↓ band. Thus, the extra electrons should be doped in the Mo4d_↓ band. Since their spins are antiparallel to the local Fe3d_↑ spins, the reduced M_s is expected, as observed.

4. SUMMARY

The influence of charge doping on the thermal diffusivity in double perovskite Sr₂FeMoO₆ by substitution of La³⁺ ions for Sr²⁺ ions is investigated. The thermal diffusivity is found to increase with La concentration, which is ascribed to the occupation of extra itinerant electrons in the down-spin Mo4d band. This result is helpful to clarify the reduced saturation magnetization M_s upon La substitution. Thus, PA and PT techniques are useful tools to investigate the micro-mechanism of the materials.

ACKNOWLEDGMENT

This work is supported by the National Natural Science Foundation of China under Grant Nos. 10374041 and 10174038, and the project-sponsored by SRF for ROCS, SEM.

REFERENCES

1. P. W. Anderson and H. Hasegawa, *Phys. Rev.* **100**: 675 (1955).
2. K. I. Kobayashi, T. Kimura, H. Sawada, K. Terakura, and Y. Tokura, *Nature* **395**: 677 (1998).
3. Y. Tomioka, T. Okuda, Y. Okimoto, R. Kumai, K. I. Kobayashi, and Y. Tokura, *Phys. Rev. B* **61**: 422 (2000).
4. F. Galasso, F. C. Douglas, and R. Kasper, *J. Chem. Phys.* **44**: 1672 (1966).
5. J. Navarro, C. Frontera, L. Balcells, B. Martinez, and J. Fontcuberta, *Phys. Rev. B* **64**: 092411 (2001).
6. Y. Moritomo, S. Xu, T. Akimoto, A. Machida, N. Hamada, K. Ohoyama, E. Nishibori, M. Takata, and M. Sakata, *Phys. Rev. B* **62**: 14224 (2000).
7. P. K. Kuo, M. J. Lin, C. B. Reyes, L. D. Favro, R. L. Thomas, D. S. Kim, and S. Y. Zhang, *Can. J. Phys.* **64**: 1165 (1986).
8. L. Guo, S. Y. Zhang, X. R. Zhang, J. He, and Z. N. Zhang, *Appl. Phys. A* **60**: 395 (1995).
9. S. W. Gerth, B. Franz, H. W. Gronert, and E. F. Wassermann, *J. Magn. Magn. Mater.* **101**: 37 (1991).
10. D. D. Sarma, P. Mahadevan, T. S. Dasgupta, S. Ray, and A. Kumar, *Phys. Rev. Lett.* **85**: 2549 (2000).
11. J. Kanamori and K. Terakura, *J. Phys. Soc. Jpn.* **70**: 1433 (2001).